



RESEARCH LETTER

10.1002/2017GL076431

Key Points:

- A global wave spectral atlas is developed and presented
- The wave spectral signature is distinct and unique at every point
- Spectral statistics provide a direct and comprehensive view of the local conditions

Correspondence to:

J. Portilla-Yandún,
jportilla@gmail.com

Citation:

Portilla-Yandún, J. (2018). The global signature of ocean wave spectra. *Geophysical Research Letters*, 45, 267–276. <https://doi.org/10.1002/2017GL076431>

Received 15 NOV 2017

Accepted 20 DEC 2017

Accepted article online 28 DEC 2017

Published online 15 JAN 2018

The Global Signature of Ocean Wave Spectra

Jesús Portilla-Yandún¹ ¹Department of Mechanical Engineering, Escuela Politécnica Nacional, Quito, Ecuador

Abstract A global atlas of ocean wave spectra is developed and presented. The development is based on a new technique for deriving wave spectral statistics, which is applied to the extensive ERA-Interim database from European Centre of Medium-Range Weather Forecasts. Spectral statistics is based on the idea of long-term wave systems, which are unique and distinct at every geographical point. The identification of those wave systems allows their separation from the overall spectrum using the partition technique. Their further characterization is made using standard integrated parameters, which turn out much more meaningful when applied to the individual components than to the total spectrum. The parameters developed include the density distribution of spectral partitions, which is the main descriptor; the identified wave systems; the individual distribution of the characteristic frequencies, directions, wave height, wave age, seasonal variability of wind and waves; return periods derived from extreme value analysis; and crossing-sea probabilities. This information is made available in web format for public use at <http://www.modemat.epn.edu.ec/#/nereo>. It is found that wave spectral statistics offers the possibility to synthesize data while providing a direct and comprehensive view of the local and regional wave conditions.

1. Introduction

It is amply accepted that knowledge of the ocean wave conditions is crucial for several marine and climate applications (e.g., navigation, ocean engineering, marine operations, coastal engineering, and climate assessment). In fact, numerous studies have been dedicated to the characterization of the wave conditions both at global and regional scales (e.g., Aarnes et al., 2017; Alves, 2006; Barstow et al., 1995; Cox & Swail, 2001; Espindola & Araujo, 2017; Semedo et al., 2011; Young & Holland, 1996; Young et al., 2011). The sources of information include in general numerical model results and observations from satellites and in situ measurements. Most of these characterization studies are based on integrated wave parameters (e.g., significant wave height H_s , mean wave period T_m , and mean wave direction θ_m). However, these descriptors are adequate only when the sea state is composed of a single wave event. On the contrary, in most cases this condition does not hold. Even in simple basins including relatively small enclosed seas, complex wave conditions have been reported (e.g., Langodan et al., 2017). In the open oceans the presence of multiple swells and wind sea is the general rule (see, e.g., Portilla-Yandún et al., 2016).

The problem is that whenever wave conditions become more complex, integrated parameters lose representation. If two or more wave systems are present, the resulting value does not faithfully correspond to any of the components. The most appreciable example is the mean wave direction (θ_m), but all the other integrated parameters are also affected. The consequence is that by considering integrated parameters only, there is a lack of insight into the physical processes and a significant loss of accuracy in the analyses. This problem has been previously recognized (e.g., Hegermiller et al., 2017), granted specially that the modern representation of wind waves is based on the concept of the wave spectrum (Pierson & Marks, 1952). This spectral representation is embedded in state-of-the-art numerical wave models and also in modern observations. This implies that the wealth amount of spectral information that is currently being gathered and produced is not fully exploited.

In this context, it is evident that progressively we need to move forward into spectral approaches for wave data analysis. Some challenges exist in this transition, some of them are technical, considering that the wave spectrum has a matrix format, more difficult to process and to visualize than scalar integrated parameters. Other challenges are practical, because most of the systems currently in place systems are designed for, and most users are accustomed to, integrated parameters. Therefore, the challenge is how to develop more comprehensive analysis methods based on the wave spectrum, compatible at the same time with current practices and methods.

Having these considerations in mind, this paper presents a methodology to serve this purpose. The method is based on the concept of spectral partitioning, which consists in identifying the subsets of the spectrum that contain a single wave system (Portilla et al., 2009). This allows making a more consistent use of integrated parameters. Partitioning facilitates also the statistical characterization of the wave spectrum, because the many dimensions of spectral data can be reduced to the parameters of major interest for particular applications. Using this methodology, and taking advantage of the large existing databases, a global atlas of wave spectral conditions has been developed and is presented here. This is certainly a more detailed approach of what has recently been published.

The data used are from the ERA-Interim archive of the *European Centre of Medium-Range Weather Forecasts* (ECMWF). The ERA-Interim data set has several advantages such as the long time span (from 1979 to present), the global coverage, and the fact that it has been extensively used and evaluated. The products of this global spectral wave climate (GLOSWAC) include long-term spectral wave descriptors, and several other characterizing parameters. These products are presented and distributed in a web format for public access. Some examples are given here to illustrate the use and interpretation of the developed information.

It is shown that spectral descriptors offer a much deeper insight into the physical processes at work in a particular area or location. Moreover, it is found that the spectral characteristics are unique at every site, becoming thus a sort of local wave spectral signature. In section 2 the data set and the applied methodology are described in more detail. In section 3 an example is developed to explain the common use of the information derived. In section 4, the analysis is expanded to a region, showing the potential for further applications. Section 5 summarizes the main results and conclusions.

2. Data Set and Methodology

2.1. The ERA-Interim Database

Any statistical characterization requires long data records, in this case of wave spectra. Depending on the use and application, these data may come from observations or model results. In the present development the interest is at global scale, not a particular point or a region. Therefore, model data are the preferred choice. Nevertheless, it is worth noting that the presented methodology is equally applicable also to observations. The ERA-Interim data set is used here because it offers several advantages. Among all the existing reanalysis databases, ERA is the only one to store spectra at each point on a global grid and at every time step (Dee et al., 2011). In fact, one of the motivations to develop this atlas is the recent public release of these data. Besides, ERA-Interim data have been extensively quality controlled and verified (e.g., Aarnes et al., 2015). Also important is the time, space, and format consistency of model data, which facilitates the processing.

The wave spectrum in ERA-Interim is discretized in 30 frequencies from 0.035 to 0.55 Hz (1.1 geometric progression) and 24 directions. The spatial grid is a reduced latitude-longitude grid with a resolution of about 110 km. This makes a total of 27,948 ocean grid points. The time span covers from 1979 to 2015 at 6 h interval, making a total of 54,056 spectra per grid point.

2.2. Spectral Partitioning

For the processing of wave spectra time series, data reduction is mandatory, specially considering that the wave spectrum comes in a matrix format that represents the variance distribution in the frequency-direction (f, θ) domain. For this, the method of spectral partitioning is used. It consists in identifying in the wave spectrum, the independent wave systems with different meteorological origin. At any specific place and time in the ocean, the wave conditions are the result of the locally generated wind waves plus swells arriving from somewhere else. All these wave systems appear distinctly in the wave spectrum as energy clusters (partitions). In practice, the partitioning algorithm treats the wave spectrum (S) as an image. This analogy facilitates its analysis by the use of image processing theory and tools.

In graph theory a partition (P_k) can be seen as a subgraph of the spectrum. It is composed of the subset of the vertices (V) and all the edges (E) , connecting pairs of vertices, that is, $S = (V, E)$. The spectrum can be then expressed as the disjoint union of the subsets P_k (equation (1)), where k is the subset number and f, θ are the vertices coordinates in the spectral space.

$$S = \bigsqcup_{k \in \mathbb{Z}} P_k = \bigcup_{k \in \mathbb{Z}} \{[(f, \theta), k] : (f, \theta) \in P_k\} \quad (1)$$

The subsets P_k are found according to the so-called mountaineer scheme. This scheme traces the steepest ascent paths from all points until a local peak is reached. This is carried out by the convolution between the vertices matrix V and the kernel H (equation (2)).

$$\begin{aligned} V'(f, \theta) &= V(f, \theta) \otimes H(i, j) \\ H(i, j) &= V \left(\max_{(i,j) \in (-1,0,1)} S(f+i, \theta+j) \right) \end{aligned} \quad (2)$$

$V'(f, \theta)$ contains the spanning tree solution, in which all points associated to the same local maximum constitute a subset or partition (P_k). All the principal and the random subsets are resolved by equation (2). However, not all of them are necessarily significant. Therefore, a postprocessing step is usually needed to discern the physically relevant features. This is done by enhancing computer vision using a filtering and thresholding sequence based on equation (3), where the kernel κ can be of the Hann or Hamming type (see Portilla et al., 2009 for details).

$$S'(f, \theta) = S(f, \theta) \otimes \kappa(i, j) \quad (3)$$

The advantage of partitioning is that the subsets can be represented by their corresponding integrated parameters (e.g., H_s^k , T_m^k , and θ_m^k), which are much more meaningful than those of the total spectrum. In addition, a significant data reduction is achieved with a marginal loss of spectral information.

2.3. Wave Spectral Statistics

Once the wave spectra are synthesized into partitions, statistical descriptors can be derived using standard procedures. The focus is on the identification of the long-term spectral wave features. Therefore, following a Bayesian approach, partitions attributes are used as spectral proxies. In this way, the multivariate spectral space can be reduced to, for example, a bivariate one. From the several possible alternatives, the empirical distribution of the peak positions (f_p^k, θ_p^k) is found to be a skillful descriptor (equation (4)); see Portilla-Yandún et al. (2015) for details.

$$\Pr(f_1 \leq F_p < f_2 | \theta_1 \leq \Theta_p < \theta_2) = \int_{\theta_1}^{\theta_2} \int_{f_1}^{f_2} g(f, \theta) df d\theta \quad (4)$$

The function $g(f, \theta)$ and the f, θ limits are obtained empirically from the long realization of spectral partitions. In turn, the long-term wave systems P_k are found using the same partitioning algorithm (equations (1) to (4)). One of the main advantages of this descriptor is the capability to reveal distinctly the wave spectral features (P_k). It turns out that these features are very specific to every location, becoming a sort of a signature of the local wave climate.

2.4. Wave Spectral Descriptors Developed in GLOSWAC

Having defined the long-term wave systems, many of their respective integrated properties can be easily derived (e.g., H_s^k , T_m^k , θ_m^k , wave age β^k , and steepness ζ^k). The partial H_s^k values are particularly relevant because they complement with energy quantification the information on recurrence present in $g(f, \theta)$. In addition, a number of other descriptors are developed within GLOSWAC. As it will soon be illustrated, together they offer a direct and comprehensive understanding of the local wave conditions.

For every point of the ERA grid these descriptors include the following: the empirical distribution of spectral partitions, $g(f, \theta)$; the long-term spectral wave systems, P_k ; the partial wave height distributions, H_s^k ; the monthly wave height mean, H_s^k ; the partial wave age distributions, β^k ; crossing-seas probabilities, $\Pr(H_s^k | H_s^m)$; the partial independent return period functions, RP_k ; the wind speed and direction distributions (wind rose); and the seasonal variability of wind speed, U_{10} .

This information is openly available from the GLOSWAC web site (<http://www.modemat.epn.edu.ec/#/nereo>). An example of its use is developed in the next section.

3. Single Point Analysis

3.1. Spectral Distribution and Long-Term Wave Systems

For illustration, the conditions at an arbitrary point are analyzed. The site is located at 72.48°W, 34.0°N in the U.S. East Coast. For this point, Figure 1 shows the descriptors available in GLOSWAC.

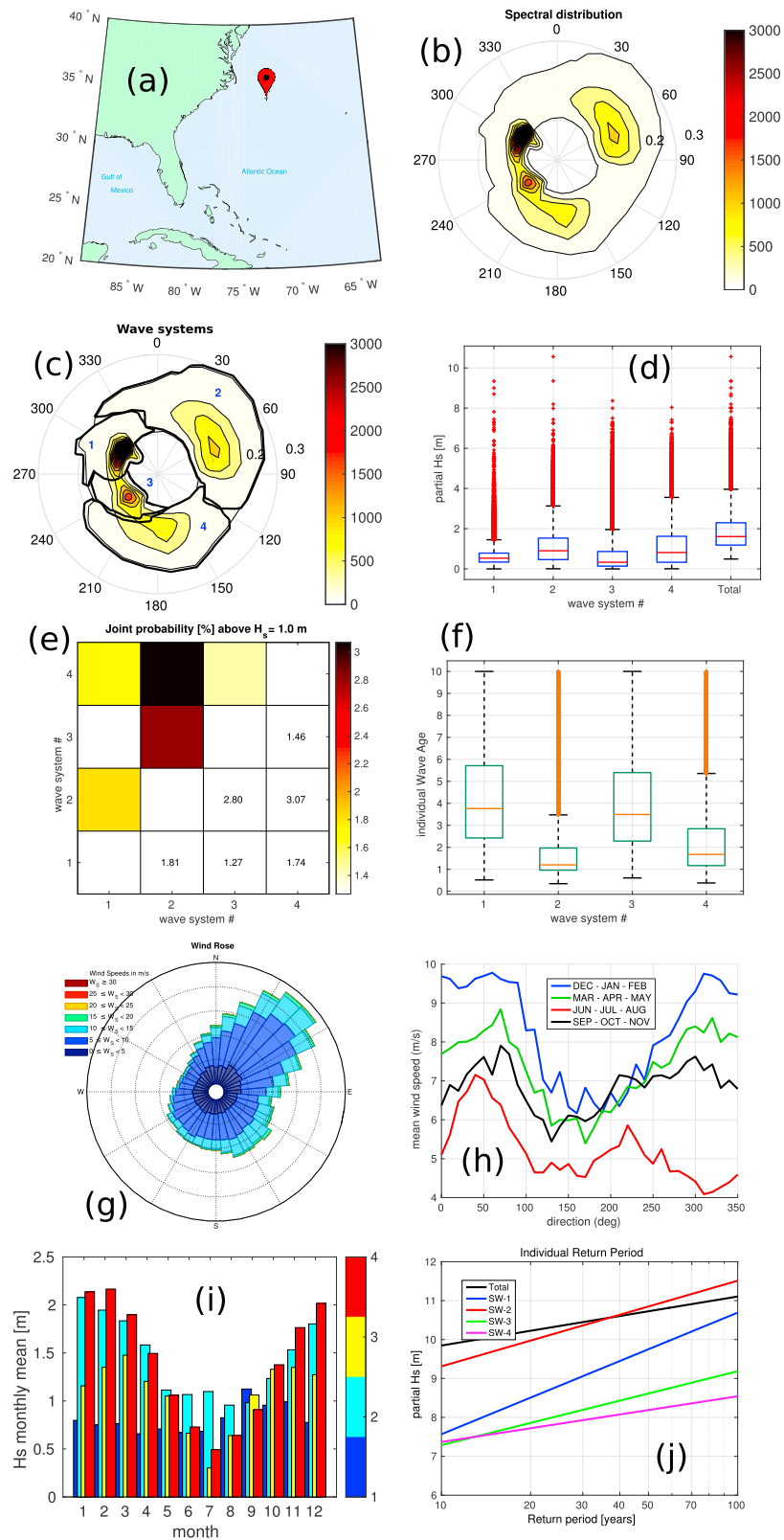


Figure 1. GLOWAC descriptors: (a) geographical location; (b) empirical distribution of spectral partitions, $g(f, \theta)$; (c) long-term spectral wave systems, P_k ; (d) partial wave height distributions, H_s^k ; (e) crossing-seas probabilities, $\Pr(H_s^k | H_s^m)$; (f) partial wave age distributions, β^k ; (g) wind speed and direction distributions (wind rose); (h) seasonal variability of wind speed, U_{10} ; (i) monthly wave height mean, H_s^k ; and (j) partial individual return periods, RP_k .

Figure 1a provides the geographical position.

Figure 1b shows the distribution of spectral partitions $g(f, \theta)$, for the period 1979–2015; the color scale indicates the number of occurrences per spectral bin. This is the most important descriptor, from which all the others are derived. It deserves thus a more detailed analysis. First of all, $g(f, \theta)$ has the same format as the spectrum $S(f, \theta)$; this is convenient as it allows a direct and consistent interpretation. In this polar representation, the radial axis correspond to frequency. Direction is specified using (flow) the oceanographic convention. Some spectral patterns and their f - θ characteristics can be readily assessed. In the example given, the cluster with the highest density is flowing to 300° . Its typical frequencies are between 0.05 and 0.2 Hz, concentrated mainly between 0.10 and 0.15 Hz. The frequency and direction spreading of this cluster are relatively low. All this suggests swell characteristics. This observation will be further verified looking at other descriptors. The information just derived is consistent with the geographical position, with swells arriving from the central Atlantic. There is another cluster flowing to 60° , its characteristic frequencies are higher than those of the previous one. Its spectral spreading is also larger; all this indicates wind sea characteristics. There are also two other spectral features to be identified. However, the purpose here is not to make a detailed analysis of the local wave conditions. More generally, the aim is to explain the information contained in the statistical indicators and how to interpret it.

The long-term spectral wave features in $g(f, \theta)$ can be automatically detected using the partitioning approach (equations (1) to (4)).

This produces the wave systems (P_k) indicated in Figure 1c. The algorithm indicates the existence of four components, whose self-consistency can be directly verified.

3.2. Partial Wave Height Distributions

Once these wave systems are detected, any of their properties can be computed from the original spectra time series. A property of immediate interest is the significant wave height H_s , because as it has been already mentioned, $g(f, \theta)$ only contains information of recurrence.

Figure 1d shows the H_s distributions for the four systems detected. For the sake of compactness these are given in a box plot format. Box plots contain basically the same information as histograms. The red line indicates the median value. The box limits indicate the 25th and 75th percentiles. The whiskers limits are placed at 1.5 the interquartile range (IQR). And the red crosses indicate extreme values, that is, the tail of the distribution. It can be seen that the first and more recurrent wave system is actually associated to relatively low H_s values (median and 75th percentile lower than 1 m). Nevertheless, it can also be seen that extreme events for this system can be 1 order of magnitude larger than its typical values. This is physically possible given the long fetch available in the Atlantic Ocean. A similar analysis can be done for the other wave systems. The last box in Figure 1d provides the distribution of the total integrated H_s value. Its characteristics deserve some attention. In this case, the magnitudes of the total H_s are larger than those of the single components. This suggests the simultaneous occurrence of more than one wave system at this location (bimodal or multimodal sea states, soon to be quantified), which cannot be assessed by looking at the total H_s only.

3.3. Crossing-Seas probabilities

As pointed out, these basic fundamental descriptors provide an insight into the spectral wave conditions. Consequently, more questions arise, like those just referred to (e.g., joint occurrence probability and state of maturity), for which specific descriptors can be and are derived. Crossing-seas conditions, for instance, are important for navigation (e.g., Cavaleri et al., 2012). They can be also associated to a larger occurrence probability of rogue waves (e.g., Toffoli et al., 2011). From integral parameters this quantification is intricate because necessarily, at least two peaks have to be identified. In addition, some arbitrary criterion needs to be set to define crossing (e.g., the angle between the peaks). With the present approach, both the wave systems (i.e., their characteristics) and their individual time series are already available. Therefore, quantifying crossing seas becomes rather straightforward. For the existing wave systems at every point, the joint occurrence probability of selected pairs can be computed (equation (5)). In GLOSWAC this is done for all possible combinations of wave systems at every point.

$$f_{x,y}(x, y) = f_{y|x}(y|x)f(x) = f_{x|y}(x|y)f(y) \quad (5)$$

where $f_{Y|X}(y|x)$ and $f_{X|Y}(x|y)$ are the conditional exceedance distributions of (H_s), Y given $X > x$, and of X given $Y > y$, respectively. $f_X(x)$ and $f_Y(y)$ are the marginal exceedance distributions for X and Y , respectively. All these variables are known from the individual time series. x and y are the corresponding variable thresholds. In GLOSWAC, the default threshold is 1.0 m for all wave systems.

The computed crossing-seas probability is given in a grid format (Figure 1e). In this representation, both axes indicate the wave system. For a particular pair, the above diagonal elements show the crossing probability in color, while the below diagonal ones provide its numeric value. It can be seen in Figure 1e that the pair 2–4 has the largest joint probability (3.07%), followed by the pair 2–3 (2.80%). In general, at this site, the joint occurrence probability of all possible pairs is relatively large. They account together for about 12% of crossing above $H_s = 1.0$ m. This reveals the complexity of the local waves, suggesting also the presence of turning wind conditions.

3.4. Partial Wave Age Distributions

Another indicator of interest is the wave age (equation (6)), which is the ratio between the wave phase speed (c_p) and the component of the wind velocity ($U_z \cos(\theta - \psi)$) in the wave propagation direction (θ).

$$\beta = \frac{c_p}{U_z \cos(\theta - \psi)} \quad (6)$$

Typically, a reference value of $\beta = 1.3$ is used to separate between wind sea and swell (e.g., Hasselmann et al., 1996). However, in reality the sea surface is a random realization of waves with different sizes, speeds, and directions. Therefore, at any particular instant each wave maintains an individual relationship with the driving wind, not considering the variability of the wind speed and direction themselves. Therefore, it is clear that β is a stochastic variable and has to be treated accordingly. On the other hand, the actual wind variable generating waves in the ECWAM model is the friction velocity (u_*) and not U_{10} as in (6). Therefore, β should be preferably expressed in terms of u_* . The use of U_{10} here is mainly user oriented, as this variable is more familiar. ($u_* = \sqrt{c_d} U_{10}$, where c_d is the drag coefficient; see, e.g., Janssen, 1991).

For each wave system, in GLOSWAC the distribution of β is given (Figure 1f), again in a box plot format. It can be seen that the wave system 2 is more related to the wind, with median β values of about 1.5 and upper quartile close to 2.0. Note, however, that the upper IQR limit is at about 3.0, but large values (10.0 or higher) do occur. Having this distribution in mind, this wave system can be labeled in a statistical sense, as wind sea. The other wave systems can be analyzed accordingly. Wave system 4 is also very much related to the wind although with slightly larger values of β . The lower quartile limit of the other two systems is above 2.0, indicating their swell nature. The case of wave system 1 was previously analyzed in terms of its f, θ characteristics. The wave age descriptor confirms its swell character. This observation can also be verified by looking at the distribution of the wind vectors, shown in the wind rose of Figure 1g. Indeed, winds in the NE sector are the most recurrent, with also high values of U_{10} (up to 20 m/s). This is followed by the sector SE. Contrarily, the NW sector (wave system 1) is associated to the lowest wind conditions. This stochastic view of the wave age is convenient for any analysis when applying equation (6). It avoids the erratic switch between wind sea and swell, typical of the variability of both wind and waves.

3.5. Wind Vectors Distribution and Seasonal Variability

Provided the long span of the data set, time variability descriptors are also developed. A seasonal view of wind and waves is provided in GLOSWAC. To facilitate the interpretation, and to be consistent with the information on waves, also, the wind direction is specified with the oceanographic convention, that is, flow direction. For wind, Figure 1h shows for the four seasons (DJF, MAM, JJA, and SON) the mean wind speed and direction. In this case it can be seen that the two preferential directions (NE and SE) prevail along the year, with some directional shift in the course of the year. Regarding waves, Figure 1i shows the monthly mean of H_s for every system. It can be clearly seen in this figure that wave systems 4 and 2 have a marked seasonality according to the boreal winter. System 3 has two peaks, one in March and other in October. In fact, the seasons JJA and SON display a high value of U_{10} in these directions (~ 240). Note that the direction of system 3 is opposite to that of system 2. Wave system 1 is relatively regular along the year, with an apparent peak in September. It is worth noting that the seasonal information just provided can be extended to include variability parameters (e.g., percentiles) not only in monthly basis but also along the years. Such information can

be used, for instance, to assess climate behavior and trends for the individual wave systems. Since waves converge from different and remote locations of the planet, they convey information from a larger area into a single point of analysis. This helps in assessing the local climate and their interconnections (e.g., Portilla-Yandún et al., 2016).

3.6. Partial Independent Return Period Functions

Finally, Figure 1j shows the individual projections of return periods for H_s derived from extreme value analysis (EVA, e.g., Coles, 2001). By looking at the distributions of H_s in Figure 1d, it is clear that the individual series have different extreme value distributions, and this is verified and displayed in Figure 1j. One of the conditions for the application of EVA is the physical and statistical independence of the events (e.g., Ochi, 1998). This condition cannot be guaranteed for the time series of the total H_s . On the contrary, the previous analysis demonstrates that there are waves from different origin and nature converging toward the site of interest. The result in this particular case is that the series of the total values produce smaller estimates, but the opposite can occur at other locations. The implications of these results in the context of EVA are significant. The projections obtained from the total values are not really trustful as they mix different populations. In turn, the individual series do not account for possible joint occurrences. Therefore, it can be concluded that a more dedicated methodology is necessary for a more precise projection of extreme wave conditions.

4. From Point Spectra to Spatial Characterization

Beyond the comprehensive analysis that can be achieved for a single point, as shown in the previous section, the use of spectral statistical indicators facilitates substantially the analysis in the spatial domain. The fact is that the space gradient of the individual wave components is rather limited from point to point (unless there is indeed a physical discontinuity, e.g., island or a sharp gradient in the meteorological forcing or bathymetry due to, e.g., the geographical configuration). Therefore, the geographical domain of the single wave features can be detected from these gradients. Note that this is a third level of data synthesization. First, the partitioning concept groups points that physically represent a *time-dependent* wave system. Second, spectral statistics hints to the existence of long-term, *time-independent*, wave systems at each point. And third, those time-independent features associated in space identify the geographical area of influence of the specific wave system. The information derived from this path of synthesization is highly self-consistent and therefore easy to interpret, because in every step there is a combined physical-statistical automated assessment. Such level of consistency cannot be attained from purely mathematical approaches, specially if only total integrated wave parameters are used.

In order to illustrate this concept, an area in the northern Indian Ocean (Arabian Sea) is analyzed (Figure 2). This area has relatively complex wave conditions with two southern swell regimes and two locally generated wave systems corresponding to the two monsoon periods (summer and winter). These four regimes can be easily identified from the spectral signature (Figure 2a). The first swell regime flows to 25° and the second to 320°. The winter monsoon flows to 200° and the summer monsoon to 80°. The corresponding magnitudes of these systems are presented in Figure 2b, showing a clear dominance of the summer monsoon. Several other characteristics can be derived at this point as it was illustrated in the previous section. However, the main interest here is the determination of the geographical domains of these wave systems.

At this purpose, the similarities of the spectral signature of each component in the study area are evaluated. Following Portilla-Yandún and Cavaleri (2016), these similarities can be quantified using the coefficient of determination (equation (7)), where S is the spectral density distribution to be evaluated for the wave system k . i refers to every grid point in the area, and o refers to the wave system proxy obtained as the expected value of S_i^k (i.e., $S_o^k = \langle S_i^k \rangle$).

$$\left(R_{o,i}^k\right)^2 = 1 - \frac{\int_{\theta} \int_r [S_i^k - S_o^k]^2 df d\theta}{\int_{\theta} \int_r [S_i^k - \overline{S_o^k}]^2 df d\theta} \quad (7)$$

The results obtained from equation (7) are presented in Figure 2. These correlation maps indicate the areas of confluence of waves with similar characteristics. Figure 2c corresponds to the swells generated in the southern storm belt that penetrate into the Indian Ocean. Note from Figure 2b that they are associated to relatively low H_s values. Also, Figure 2d corresponds to swells, in this case generated by the trade winds crossing the

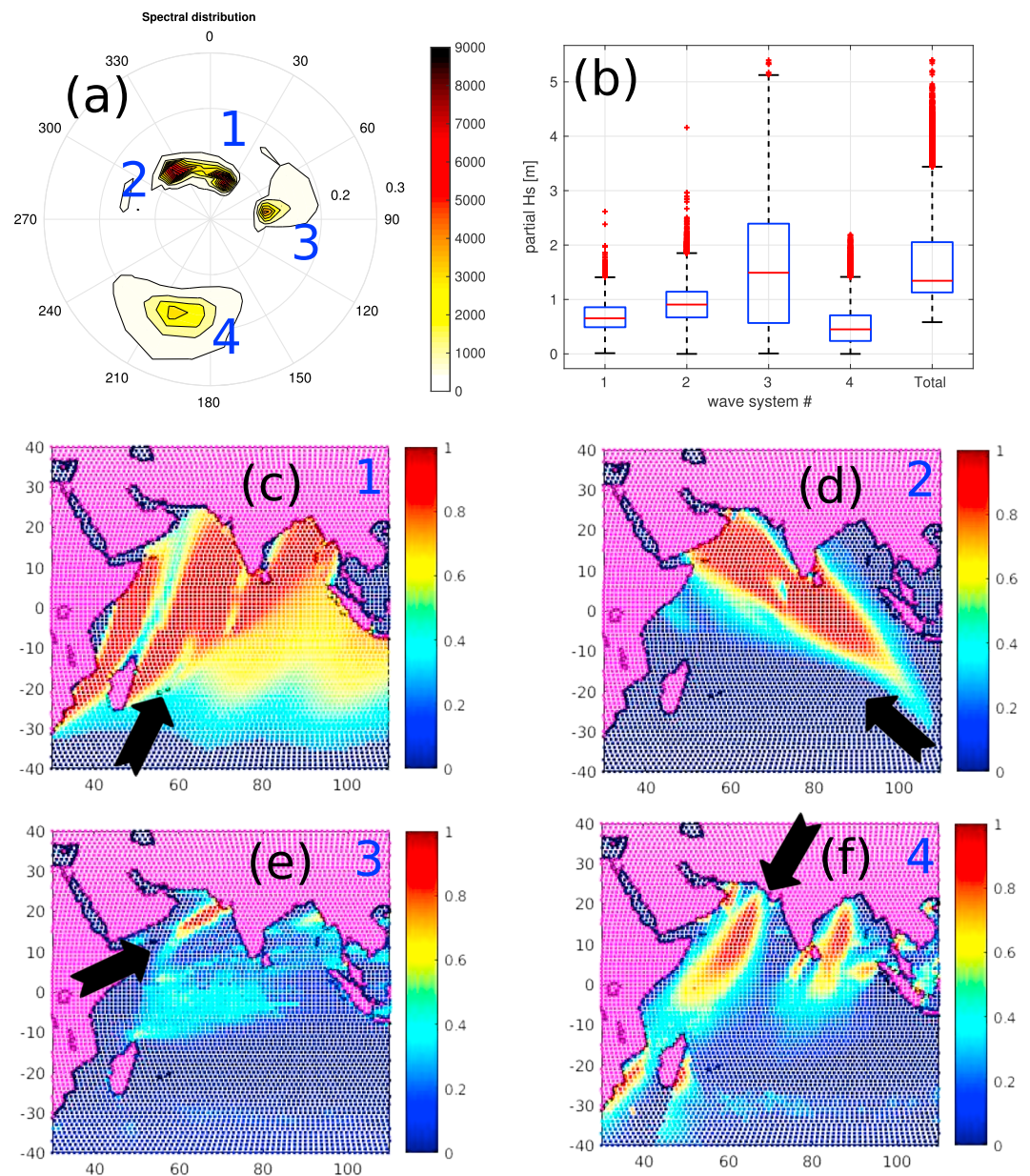


Figure 2. Spatial distribution of the main wave regimes in the Arabian Sea (65.73°E , 10°N), (a) distribution of spectral partitions, and (b) partial wave height distributions. (c) Swells from the southern storm belt, (d) swells from the easterly trade winds, (e) summer monsoon, and (f) winter monsoon.

region from south east (Australian region). Figure 2e shows the area of influence of the summer monsoon, which according to Figure 2b are the most dominant conditions in terms of magnitude. Figure 2f shows the correlation of wave conditions for the winter monsoon regime. As can be seen, these waves can travel far south into the Indian Ocean, albeit with progressively smaller magnitudes. The determination of the spatial domains of wave systems opens new possibilities for wave data analysis yet to be explored, including climate assessment, strategic mooring deployment, a more precise computation of background errors for inverse modeling, and wave data assimilation.

5. Summary, Conclusions, and Perspectives

In this study two important developments are put together: on the one hand, a modern technique to derive wave spectral statistics presented in Portilla-Yandún et al. (2015) and on the other hand, the application of

this technique to global-scale data from the ERA-Interim database, which became publicly available since 2015. This allows the development of a world wave spectral atlas (GLOSWAC). This atlas is available online for public use and contains a set of wave parameters that together provide a direct and comprehensive interpretation of the world wave climate with an insight in the spectral characteristics.

Wave spectral statistics are based on the idea of long-term wave systems at every geographical point. These wave systems are defined in terms of the density distribution of spectral partitions. It is found that this distribution is unique at every point and therefore constitutes a sort of local wave spectral signature. Once these systems are identified, their description can be made using standard wave parameters per individual component. Several parameters are included in GLOSWAC. Apart from the distribution of the characteristic frequencies and directions, inherent to the spectral distribution, the atlas includes wave height, wave age, seasonal variability of wind and waves, return periods derived from extreme value analysis, and crossing-sea probabilities. An example is presented here to illustrate the use of this information at any reference point.

By exploring the world wave characteristics using this tool, it can be observed that most world locations are characterized by complex spectral wave conditions, with bimodal or multimodal characteristics even in places thought to be driven by relatively simple meteorological conditions. In some cases, the magnitude of the wave systems can be relatively low so they tend to be overlooked when using total integrated parameters. Nevertheless, several types of analysis require independent series for statistical inference and prediction. This separation is crucial, for instance, in extreme value analysis or in the identification of regions of significant crossing-seas probabilities. It is also shown that the separation of wave systems allows to define other parameters in statistical terms. This is the case of the wave age involved in the conception of different types of waves according to the wind forcing, wind sea, and swell.

Wave spectral statistics opens a new dimension for wave data analysis. This method allows exploiting the large amount of spectral information already available. It also offers the possibility of data reduction while keeping the most substantial spectral information. A direct application is the identification and description of the world ocean wave fields, of which an example is worked out here for the Indian Ocean. Several new possibilities are derived from these individual fields including climate analysis, strategic mooring deployment, and a more precise computation of background errors for inverse modeling and wave data assimilation.

This new methodology and the information derived allow also a cross verification among different data sources, for instance, between different model sources or between model data and observations such as in situ or satellite data. The scope here is limited to the development of a world atlas taking advantage of ERA-Interim, but as new information becomes available from monitoring networks, and equipped remote sensors such as SAR (*Synthetic Aperture Radar*), different sources of information can be validated at spectral level.

Acknowledgments

This work was funded by Escuela Politécnica Nacional (project PIJ-1503) and supported by ModeMat-EPN (Centro de Modelización Matemática). Part of this work was done during research visits to ISMAR-CNR in Venice (Italy) and KAUST University (Saudi Arabia). I am very grateful to Luigi Cavaleri, Ibrahim Hoteit, and Sabique Langodan for the interaction and useful comments during these visits. The collaboration of Jeison Sosa, Andrés Salazar, Cristhian Valladares, and Edwin Jácome is highly appreciated. I am also grateful to Brian Blaton for providing the *read_grib* software and also for his prompt support. This development was possible by the public release of the ERA-Interim spectral data by ECMWF. In particular, Jean Bidlot provided guide and support with data processing. The dedicated work of the anonymous reviewers helped improve the final quality of the manuscript.

References

- Aarnes, O. J., Abdalla, S., Bidlot, J., & Breivik, Ø. (2015). Marine wind and wave height trends at different ERA-Interim forecast ranges. *Journal of Climate*, 28(2), 819–837. <https://doi.org/10.1175/JCLI-D-14-00470.1>
- Aarnes, O. J., Reistad, M., Breivik, Ø., Bitner-Gregersen, E., Ingolf Eide, L., Gramstad, O., ... Vanem, E. (2017). Projected changes in significant wave height toward the end of the 21st century: Northeast Atlantic. *Journal of Geophysical Research: Oceans*, 122, 3394–3403. <https://doi.org/10.1002/2016JC012521>
- Alves, J. H. G. M. (2006). Numerical modeling of ocean swell contributions to the global wind-wave climate. *Ocean Modelling*, 11, 98–122. <https://doi.org/10.1016/j.ocemod.2004.11.007>
- Barstow, S. F., Haug, O., & Krogstad, H. E. (1995). World wave atlas: A PC MS-WINDOWS product for wave climate assessment globally. In *Proceedings of the 3rd Thematic Conference on Remote Sensing for Marine and Coastal Environments* (Vol. 1, pp. 95–103). Seattle: Environmental Conservation.
- Cavaleri, L., Bertotti, L., Torrisi, L., Bitner-Gregersen, E., Serio, M., & Onorato, M. (2012). Rogue waves in crossing seas: The Louis Majesty accident. *Journal of Geophysical Research*, 117, C00J10. <https://doi.org/10.1029/2012JC007923>
- Coles, S. (2001). *An Introduction to Statistical Modeling of Extreme Values*. London: Springer. <https://doi.org/10.1007/978-1-4471-3675-0>
- Cox, A. T., & Swail, V. R. (2001). A global wave hindcast over the period 1958–1997: Validation and climate assessment. *Journal of Geophysical Research*, 106, 2313–2329. <https://doi.org/10.1029/2001JC000301>
- Dee, D. P., Uppala, S. M., Simmons, A. J., Berrisford, P., Poli, P., Kobayashi, S., ... Vitart, F. (2011). The ERA-Interim reanalysis: Configuration and performance of the data assimilation system. *Quarterly Journal of the Royal Meteorological Society*, 137, 553–597. <https://doi.org/10.1002/qj.828>
- Espindola, R. L., & Araujo, A. M. (2017). Wave energy resource of Brazil: An analysis from 35 years of ERA-Interim reanalysis data. *PLoS ONE* 12(8), e0183501. <https://doi.org/10.1371/journal.pone.0183501>
- Hasselmann, S., Brüning, C., Hasselmann, K., & Heimbach, P. (1996). An improved algorithm for the retrieval of ocean wave spectra from synthetic aperture radar image spectra. *Journal of Geophysical Research*, 101, 16,615–16,629. <https://doi.org/10.1029/96JC00798>

- Hegermiller, C. A., Antolinez, J. A. A., Rueda, A., Camus, P., Perez, J., Erikson, L. H., ... Mendez, F. J. (2017). A multimodal wave spectrum-based approach for statistical downscaling of local wave climate. *Journal of Physical Oceanography*, 47(2), 375. <https://doi.org/10.1175/JPO-D-16-0191.1>
- Janssen, P. A. (1991). Quasi-linear theory of wind-wave generation applied to wave forecasting. *Journal of Physical Oceanography*, 21(11), 1631–1642. [https://doi.org/10.1175/1520-0485\(1991\)021%3C1631:QLTOWW%3E2.0.CO;2](https://doi.org/10.1175/1520-0485(1991)021%3C1631:QLTOWW%3E2.0.CO;2)
- Langodan, S., Cavaleri, L., Pomaro, A., Vishwanadhapalli, Y., Bertotti, L., & Hoteit, I. (2017). The climatology of the Red Sea—Part 2: The waves. *International Journal of Climatology*, 37(13), 4518–4528. <https://doi.org/10.1002/joc.5101>
- Ochi, M. K. (1998). *Ocean Waves: The Stochastic Approach*. New York: Cambridge University Press. <https://doi.org/10.1017/CBO9780511529559>
- Pierson, W. J., & Marks, W. (1952). The power spectrum analysis of ocean-wave records. *Eos, Transactions American Geophysical Union*, 33(6), 834–844. <https://doi.org/10.1029/TR033i006p00834>
- Portilla, J., Ocampo-Torres, F., & Monbaliu, J. (2009). Spectral partitioning and identification of wind sea and swell. *Journal of Atmospheric and Oceanic Technology*, 26(1), 107–122. <https://doi.org/10.1175/2008JTECHO609.1>
- Portilla-Yandún, J., & Cavaleri, L. (2016). On the specification of background errors for wave data assimilation systems. *Journal of Geophysical Research: Oceans*, 121, 209–223. <https://doi.org/10.1002/2015JC011309>
- Portilla-Yandún, J., Cavaleri, L., & Van Vledder, G. P. (2015). Wave spectra partitioning and long term statistical distribution. *Ocean Modelling*, 96(Part 96), 148–160. <https://doi.org/10.1016/j.ocemod.2015.06.008>
- Portilla-Yandún, J., Salazar, A., & Cavaleri, L. (2016). Climate patterns derived from ocean wave spectra. *Geophysical Research Letters*, 43, 11,736–11,743. <https://doi.org/10.1002/2016GL071419>
- Semedo, A., Sušelj, K., Rutgersson, A., & Sterl, A. (2011). A global view on the wind sea and swell climate and variability from ERA-40. *Journal of Climate*, 24(5), 1461–1479. <https://doi.org/10.1175/2010JCLI3718.1>
- Toffoli, A., Bitner-Gregersen, E. M., Osborne, A. R., Serio, M., Monbaliu, J., & Onorato, M. (2011). Extreme waves in random crossing seas: Laboratory experiments and numerical simulations. *Geophysical Research Letters*, 38, L06605. <https://doi.org/10.1029/2011GL046827>
- Young, I. R., & Holland, G. J. (1996). *Atlas of the Oceans: Wind and Wave Climate, Atlas* (p. xvi). Oxford, New York and Tokyo: Pergamon/Elsevier Science Ltd.
- Young, I. R., Zieger, S., & Babanin, A. V. (2011). Global trends in wind speed and wave height. *Science*, 332, 451. <https://doi.org/10.1126/science.1197219>